Annu. Rev. Genomics Hum. Genet. 2001. 2:271–97
Copyright © 2001 by Annual Reviews. All rights reserved

USHER SYNDROME: From Genetics to Pathogenesis

Christine Petit
Unité de Génétique des Déficits Sensoriels, CNRS URA 1968 Institut Pasteur, 75724 Paris, Cedex 15, France; e-mail: cpetit@pasteur.fr

Key Words syndromic deafness, retinitis pigmentosa, sensory cell disease, photoreceptor cells, hair cells, lateral links, cell-cell junctions, unconventional myosin, PDZ domain–containing protein, cadherin-like protein, planar polarity

■ **Abstract** Usher syndrome (USH) is defined by the association of sensorineural deafness and visual impairment due to retinitis pigmentosa. The syndrome has three distinct clinical subtypes, referred to as USH1, USH2, and USH3. Each subtype is genetically heterogeneous, and 12 loci have been detected so far. Four genes have been identified, namely, *USH1B*, *USH1C*, *USH1D*, and *USH2A*. *USH1B*, *USH1C*, and *USH1D* encode an unconventional myosin (myosin VIIA), a PDZ domain–containing protein (harmonin), and a cadherin-like protein (cadherin-23), respectively. Mutations of these genes cause primary defects of the sensory cells in the inner ear, and probably also in the retina. In the inner ear, the *USH1* genes, I propose, are involved in the same signaling pathway, which may control development and/or maintenance of the hair bundles of sensory cells via an adhesion force (*a*) at the junctions between these cells and supporting cells and (*b*) at the level of the lateral links that interconnect the stereocilia. In contrast, the molecular pathogenesis of USH2A, which is owing to a defect of a novel extracellular matrix protein, is likely to be different from that of USH1.

INTRODUCTION

Over 400 syndromes with deafness as one of the symptoms have been described in the literature (46). They include a vast ensemble of hereditary monogenic diseases in which hearing loss is associated with miscellaneous disorders of the musculoskeletal, cardiovascular, urogenital, nervous, endocrine, digestive, or integumentary systems. About 40 of these syndromes include an ocular disorder (45). Among them is Usher syndrome (USH), defined by a bilateral sensorineural deafness that originates in the cochlea (the auditory sensory organ) and a loss of vision due to retinitis pigmentosa. This syndrome is the most frequent cause of deafness accompanied by blindness. It accounts for more than 50% of individuals who are both deaf and blind (142), about 18% of retinitis pigmentosa cases, and 3%–6% of congenital deafness cases (20). Its prevalence is between 1/16,000 and 1/50,000, based on studies of Scandinavian (48, 51, 84, 104, 120), Columbian (132), British (57), and American populations (20); for individuals between the ages of 30 and 49, the prevalence approaches 1/10,000 (57).

1527-8024/01/0728-0271$14.00

As early as 1858, the occurrence of a pigmentary retinopathy with deafness was observed in three siblings (out of a total of five) by the German ophthalmologist Alfred von Graefe and reported by his cousin Albrecht von Graefe (144). This discovery was made possible by the invention of the ophthalmoscope by German optical physiologists during the mid-nineteenth century (21). In 1861, Liebreich reported a survey of deaf inhabitants from Berlin in whom he noted the frequent presence of retinal pigmentation, in particular in Jewish consanguineous families (83). The existence of this dual sensory defect had been documented by several other reports, and its hereditability was well established when, in 1914, Charles Usher, a British ophthalmologist, looked at the incidence of deafness in 69 cases of retinitis pigmentosa (140). Following the description of the clinical heterogeneity of the syndrome, which was already outlined in the initial reports (12, 51), a classification into three subtypes, Usher type I (USH1), type II (USH2), and type III (USH3), was proposed in 1977 by Davenport & Omenn (31). During the 1990s, each of these clinical forms was shown to be genetically heterogeneous.

The study of USH may offer a unique opportunity to decipher the molecular bases of some of the developmental and functional similarities existing between the retinal and the cochlear sensory cells, i.e., the photoreceptor cells and the hair cells. Indeed, at least in some genetic forms of the disease, these cells have been shown to be the primary targets of the gene defect. What are the main structural features common to the photoreceptor cells (Figure 1) and the auditory hair cell (Figure 2)? First, both are ciliated cells: Photoreceptors possess a connecting cilium situated in a segment that links the internal segment to the external segment; embryonic auditory hair cells have an apical cilium, the kinocilium, which disappears soon after birth in mammals. Second, both cell types possess microvillar structures. In vertebrates, photoreceptors contain lamellar structures, forming discs where the phototransduction occurs; in invertebrates, discs are replaced by rhabdomeres, which are tightly packed genuine microvilli. The apical part of auditory hair cells carries up to 300 rigid microvilli, improperly named stereocilia, where the mechanotransduction takes place. Third, the synapses of both photoreceptors and auditory sensory cells have special characteristics: They are called ribbon synapses in reference to their plate-like presynaptic bodies to which synaptic vesicles are tethered. From a functional point of view, these synapses are characterized by a massive, rapid, and sustained discharge of neurotransmitters (147). Finally, the molecular analysis of Usher syndrome may also lead to the discovery of novel biological processes shared by cochlear and retinal sensory cells.

THREE CLINICAL SUBTYPES

The clinical classification of Usher syndrome, established by Davenport & Omenn is still in use (31). USH1 is the most severe form. It is characterized by severe to profound congenital sensorineural deafness, constant vestibular dysfunction (balance deficiency), and prepubertal onset retinitis pigmentosa. Vestibular dysfunction manifests clinically as a delay in motor development. Affected children cannot sit without support at 6 months of age and often do not walk before 18 months (100, 127). An ataxia of vestibular origin is occasionally observed. The retinopathy appears as a loss of night vision and a restriction of the visual field during childhood, and eventually, as a visual acuity loss that rapidly progresses to blindness. Anomalies of light-evoked electrical response of the retina can be detected as soon as 2 to 3 years of age by electroretinography, thus permitting early diagnosis of the disease. Later, fundus anomalies develop, which consist of pigment deposition likened to bone spicules around mid-periphery of the retina, thereafter extending inward and outward, and a narrowing of blood vessels. USH2 is mainly distinguished from USH1 by a less severe deafness, i.e., a mild hearing loss for low frequency sounds and a severe hearing loss for high frequency sounds, with the absence of the vestibular dysfunction. The loss of night vision develops around puberty (the age of onset partly overlaps that of USH1). The progression of the visual impairment seems to present a higher variability than in USH1 (145). Patients usually have fundoscopic anomalies beyond childhood (72). A third type, USH3, has been described as distinct from USH2 because of the progressiveness of the hearing loss and the occasional presence of vestibular dysfunction (47, 67, 68). In each of these forms, retinitis pigmentosa can be accompanied by cataract (9).

Initially, the respective proportions of USH1 and USH2 cases were reported to be 90% and 10% (51). This evaluation, however, was biased, as the examined patients were severely to profoundly deaf. In more recent analyses of patients from the United States and Northern Europe, USH1 and USH2 were reported between 33% and 44% and between 56% and 67%, respectively (38, 57, 108, 120). In Colombia however, 70% of the USH cases have been diagnosed as USH1 (132), a likely overestimated value as it is based on the screening of individuals attending schools for the deaf (whereas the degree of hearing loss of USH2 allows for a normal schooling). USH3 had first been evaluated at a very low percentage (31). Subsequently, the existence of this form was considered uncertain (127). The finding of USH3 in Finland, where it is the most common form of Usher syndrome (40% of cases) (107), due to a founder effect in this population, definitively established the reality of this form. Recently, USH3 was reported to account for 20% of the USH cases in the city of Birmingham (United Kingdom) (57).

Although the histopathological data on the syndrome are sparse and often related to undefined USH subtypes, examination of the temporal bone has been documented in some cases (131, 146). Whatever the supposed USH subtype, a severe degeneration of the organ of Corti (the auditory sensory epithelium) was observed, at least in the basal turn of the cochlea. The cochlear ganglion (devoted to afferent innervation) was atrophied. In USH1, the structure of the vestibular end organs varied from normal to a severe degeneration of certain neuroepithelial areas. No vestibular anomaly was detected in USH2 and USH3. In several patients affected by an undefined USH subtype, ciliar anomalies have been reported of both the connecting cilium of photoreceptor cells (11, 18, 60) and the cilium of olfactory receptor neurons (7). Slow sperm motility and an abnormal structure of the sperm cilium have also been described and proposed to account for patients' decreased fertility (60). Finally, bronchiectasis and reduced nasal mucociliary clearance, which were observed in some USH1 patients, might also be related to a ciliar dysfunction (18). Recently, sperm anomalies have been sought in USH2A patients, but no anomaly of the cilium could be detected (141); it is thus tempting to ascribe the reported ciliar anomalies to the USH1 form.

LOCI IDENTIFICATION*

The first USH locus to be mapped was USH2A, for Usher type II, in 1990. It was assigned to the distal part of chromosome 1q through the study of affected families from the United States and Europe (74). Next, the USH1A locus was found by analysis of a population from Poitou-Charentes, in the west of France (66); this locus has only been detected in this population so far. The first locus for USH3 was reported in 1995, in Finnish families (122). At present, evidence for 12 distinct genetic loci for Usher syndrome has been obtained (see Table 1), namely, 6 loci for USH1, USH1A at 14q32 (MIM 276900) (66), USH1B at 11q13.5 (MIM 276903) (73, 128), USH1C at 11p15.1 (MIM 276904) (128), USH1D at 10q (MIM 601067) (149), USH1E at 21q21 (MIM 602097) (24), USH1F (MIM 602083) on chromosome 10 (150); 4 loci for USH2, USH2A at 1q41 (MIM 276901) (74, 82), USH2B at 3p23-24.2 (MIM 276905) (56), USH2C at 5q14.3-21.3 (MIM 605472) (109), and a fourth locus not yet defined (156); 2 loci for USH3, USH3A (MIM 276902) at chromosome 3q21-25 (122) and 1 locus on the long arm of chromosome 20 (M. Mustapha, D. Weil, S. Chardenoux, R. Slim, & C. Petit, unpublished data). Of these 12 genetic forms, which all are transmitted on the autosomal recessive mode, USH1B and USH2A are the most prevalent. The former accounts for 30% to 60% of the USH1 cases (2, 8, 15, 63), the latter, for 74% to 82% of the USH2 cases (110, 156).

THE *USH* GENES

USH1B

The gene responsible for Usher 1B (*USH1B*) was the first USH gene to be isolated. This cloning was greatly facilitated by the study of the *shaker-1* (*sh-1*) mouse mutants (32, 118). Indeed, the *sh-1* phenotype had been assigned to the murine chromosomal region homologous to that defined for USH1B (22). *Sh-1*

---

*Disease loci and genes are referenced according to the Online Mendelian Inheritance in Man (OMIM) website nomenclature, (http://www.ncbi.nlm.nih.gov/Omim/searchomim.html).

TABLE 1 The genetic forms of Usher syndrome

Usher form	Chromosomal localization	Gene	Protein	DFNA/DFNB form	Mouse model
USH1A	14q32 (66)	—	—	—	—
USH1B	11q13.5 (73, 128)	*MYO7A* (152)	Myosin VIIA	DFNB2 (87, 153) DFNA11 (88)	*shaker-1* (42)
USH1C	11p15.1 (128)	*USH1C* (16, 143)	Harmonin	DFNB18?	—
USH1D	10q (149)	*CDH23* (17, 19)	Cadherin23	DFNB12 (19)	*waltzer* (33)
USH1E	21q21 (24)	—	—	—	—
USH1F	10 (150)	PCDH15 (4a)	Protocadherin15	DFNB23?	*Ames waltzer* (5)
USH2A	1q41 (74, 82)	*USH2A* (38)	Usherin	—	—
USH2B	3p23-24.2 (56)	—	—	DFNB6?	—
USH2C	5q14.3-21.3 (109)	—	—	—	—
USH3A	3q21-25 (122)	—	—	—	—

Princeps references are given.

mice exhibit head-tossing, circling behavior, and hyperactivity due to vestibular dysfunction. A rapidly progressive hearing loss accompanied by degeneration of the organ of Corti (70) is also exhibited. Although a lack of retinal degeneration had been reported in these mutants, the *sh-1* phenotype was hypothesized to involve the *USH1B* orthologue. A positional cloning strategy led to the identification of the murine *Myo7a* gene, predicted to encode the unconventional myosin VIIA, in the *sh-1* candidate interval. Because experimental evidence already supported a role of unconventional myosins in the auditory mechanotransduction process (43, 58), the myosin VIIA gene was considered a promising candidate for both *sh-1* and USH1B. Indeed, mutations in exons encoding the motor head of myosin VIIA were detected concurrently in *sh-1* mice (42) and in USH1B patients (152).

MYO7A consists of 48 coding exons (17 for the head, 3 for the neck, and 28 for the tail of the molecule) and encodes several alternatively spliced forms, mainly differing in their motor head. It extends over 100 kb (27, 154). Since the original report in 1995, a total of 81 different mutations have been detected in USH1B patients. They are distributed all along the gene, although somewhat clustered in the part encoding the motor head (2, 15, 29, 30, 37, 63, 81, 91, 152, 155, 157). About half of the mutations are missense or in-frame insertions/deletions. There is no indication for a hot spot of mutations. Of the 10 *sh-1* alleles, 7 have been analyzed; the mutations have roughly the same distribution and characteristics as the human mutations (42, 54, 96). Interestingly, among the category of zebrafish *circler* mutants that are characterized by defective hair cells of the auditory-vestibular and lateral line systems (i.e., two likely homologous sensory systems) (102), the five alleles of the *mariner* class carry *myo7a* mutations (36).

Unconventional myosins form a large family that is presently divided into 16 classes (14a). These motor proteins move along the actin filaments by using the energy generated by the hydrolysis of ATP. Their highly conserved N-terminal motor head possesses the actin- and ATP-binding sites. It is followed by a neck region and a tail that is highly divergent from one myosin to another. The tail sequence determines the functional specificity of each myosin, as it contains various putative protein-protein interacting domains that bind to cargo molecules, regulatory factors, and components of the transduction pathways (14a). Unconventional myosins have been implicated in the formation and the movements of cytoplasmic expansions, in the movements of vesicles, the transport of mRNA, and in signal transduction (14a, 92, 97, 135). The human myosin VIIA (Figure 3), 2215 amino acids in length (254 kDa), consists of a motor head domain of 729 amino acids, containing the ATP- and actin-binding motifs; a neck region of 126 amino acids, composed of five IQ (isoleucine-glutamine) motifs that are expected to bind calmodulin; and a long tail of 1360 amino acids (154). The actin-based motility of the head was demonstrated recently (139). The tail begins with a short coiled-coil domain (78 amino acids) that mediates the formation of homodimers (153). The coiled-coil domain is followed by two large repeats of about 460 amino acids. Each repeat contains a MyTH4 (myosin tail homology 4) domain, of unknown function, and a domain homologous to the membrane-binding domain of the proteins of the FERM (4.1, ezrin, radixin, moesin) superfamily (28). The tandem association of

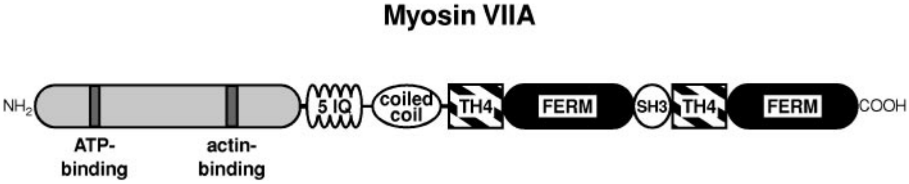

Figure 3 Schematic representation of myosin VIIA. This unconventional myosin consists of a motor head that contains the ATP- and actin-binding sites, a neck region composed of five isoleucine-glutamine (IQ) motifs expected to bind calmodulin, and a long tail of 1360 amino acids. The tail begins with a short coiled-coil domain, which is implicated in the formation of homodimers. The coiled-coil domain is followed by two large repeats, each containing a MyTH4 (myosin tail homology 4) and a FERM (4.1, ezrin, radixin, moesin) domain. The two repeats are separated by a poorly conserved SH3 (src homology-3) domain.

the MyTH4 and FERM domains, which is also present in myosin V, myosin XV, and a plant kinesin (14a, 27, 115, 148), argues in favor of a functional significance for this pairing. These two repeats are separated by a poorly conserved SH3 (src homology 3) domain (27, 96), a type of domain known to interact with proline-rich regions (101).

USH1C

In 1966, Kloepfer reported an unusually high frequency of USH patients in a small population of southwestern Louisiana who were descendents of French-speaking emigrants exiled from Acadia (Canada) in the eighteenth century (75). In 1994, this form was individualized as USH1C by linkage analysis and, for a long time, has only been observed in patients related to this community (10, 69, 128). The gene underlying USH1C was recently isolated using two different strategies, namely, a candidate gene approach (based on a subtracted cDNA library derived from microdissected sensory areas of the vestibular end organs) (143) and a positional cloning strategy (based on the analysis of a chromosomal deletion underlying a contiguous gene syndrome) (16). *USH1C* encodes a PDZ domain–containing protein, termed harmonin; it consists of 28 coding exons and spans about 51 kb (16, 143). So far, six mutations have been reported (16, 143, 163), none of which is a missense mutation. Which mutation(s) cause the disease in the Acadian affected individuals is still not clear. Indeed, two distinct causative mutations have been reported, namely, an expanded intronic VNTR proposed to affect transcriptional and/or posttranscriptional processes (143) and an exonic substitution that is consistent with the creation of a new splice site and leads to a small in-frame deletion and an unstable transcript (16). One mutation, 238-239insC, was detected in several European individuals (143) who share a common haplotype, thus arguing in favor of a founder effect (163). Mutation screening in a German population provided a minimal estimation of 12.5% of *USH1C* mutations among USH1 cases (163).

USH1C encodes a variety of alternatively spliced transcripts that result from the differential use of eight exons. In the murine inner ear, these transcripts predict at least eight harmonin isoforms, ranging from 420 to 910 amino acids in length (143). They can be distributed into three subclasses according to the number of domains they contain, namely, two or three PDZ domains, one or two coiled-coil domains, and the presence/absence of a PST (proline, serine, threonine) domain (Figure 4). The coiled-coil domain(s) might be implicated in the dimerization of the protein. Proline-rich domains serve as binding sites for SH3, WW (trp-trp), EVH1 [*Drosophila* enabled/VASP (vasodilator-stimulated phosphoprotein) homology 1] domains (129), and the actin-regulatory protein profilin (65, 98). PDZ domains are interacting domains, 80 to 90 amino acids in length, originally detected in PSD/SAP90 (postsynaptic density protein), Dlg-A (*Drosophila* tumor suppressor), and ZO-1 (tight junction protein). The PDZ domain–containing proteins form a vast class of molecules, with one representative in bacteria (111). They are central organizers of high-order supramolecular complexes located at

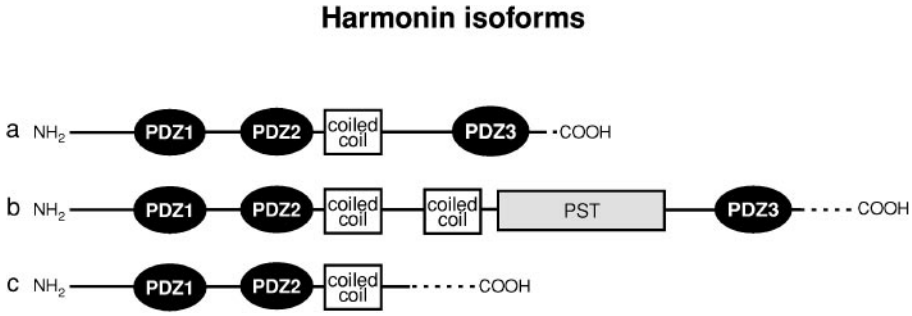

Figure 4 Schematic representation of the three predicted classes of harmonin isoforms. Class a isoforms contain three PDZ domains and one coiled-coil domain between PDZ2 and PDZ3. Class b isoforms contain an additional coiled-coil domain and a proline, serine, threonine (PST)-rich region. Class c isoforms contain only the first two PDZ domains and the first coiled-coil domain. Each class has two or three predicted isoforms, which differ in their internal sequences (class a) or in their C-terminal ends (class b and class c) [adapted from Verpy et al (143)].

specific emplacements of the plasma membrane. They bind not only to transmembrane proteins, in particular, ionic channels or transporters (50, 71, 126), but also to actin or actin-binding proteins. Hence, they cluster and coordinate the activity of various plasma membrane proteins and bridge them to the cortical cytoskeleton (39, 41, 125).

USH1D

The USH1D locus was defined by the study of a Pakistani family (149). The gene was recently isolated independently by two groups. One discovery was the result of a collaborative study aimed at identifying the gene defect underlying the phenotype of the *waltzer* (v) deaf mouse mutants (17). Indeed, based on mapping data (23, 162), these mutants had been proposed as the mouse model for USH1D, even though no retinal anomaly has been observed in these mice (5). The other group found the USH1D gene by a direct positional cloning strategy (19). This gene, *CDH23* (MIM 605516), comprises 69 coding exons and spans more than 300 kb (17). It encodes a cadherin-related protein.

Eight distinct mutations have been reported, namely, two nonsense mutations, one single-codon deletion, one missense mutation, three splice-site mutations that are predicted to preserve the reading frame, and one truncating splice-site mutation (17, 19). In the three *v* mutants analyzed, a nonsense and two splice-site mutations were found (33). USH1D seems to be the second most common genetic form of USH1 (8). Interestingly, individuals homozygous for the *CDH23* missense mutation present with a mild form of retinitis pigmentosa (almost undetectable in one patient) (17). A mild retinopathy was also observed in a family with a splice-site mutation preserving the reading frame (17).

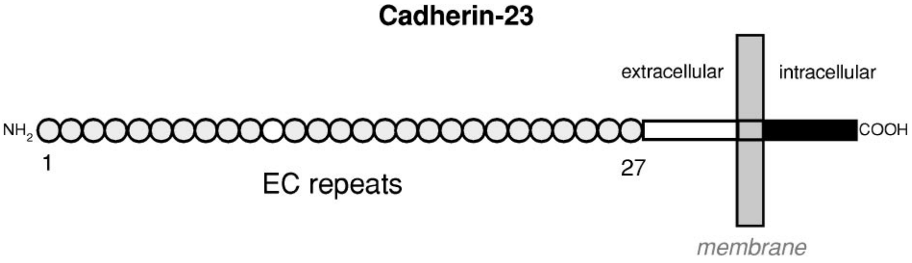

Figure 5 Schematic representation of cadherin-23. The protein ectodomain is composed of 27 extracellular cadherin (EC) repeats. The predicted cytoplasmic region (268 residues) has no homology with known proteins.

The predicted protein (Figure 5), termed cadherin-23, is composed of 3354 amino acids (17). Its ectodomain is composed of 27 extracellular cadherin (EC) repeats (17), most of which possess the characteristic Ca^{2+}-binding motifs of cadherins. These motifs are implicated in the calcium-dependent interaction between cadherins, which mediates cell-cell adhesion. The single transmembrane domain is followed by a 268 amino acid cytoplasmic region (17, 19). Cadherin-23 is more closely related to the subgroup of cadherins defined by the Drosophila fat, dachsous, and the human MEGF1 proteins, which are characterized by a large number of EC repeats (103, 161). However, its intracytoplasmic part shows no homology with known proteins. In particular, no clear β-catenin–binding motif can be detected.

USH2A

The gene underlying USH2A has been isolated by a positional cloning strategy; it comprises 21 exons, with the first exon being entirely noncoding (38). *USH2A* encodes a predicted 1551 amino acid (171 kDa) protein. This protein (Figure 6) begins with a signal peptide and has a modular structure. It is composed of a N-terminal 285 amino acid unclassified domain, followed by a laminin domain VI module (about 200 residues) (156), a tandem array of 10 laminin-type EGF-like (LE) modules, and four fibronectin-like type III (F3) repeats. Of particular interest are the other types of proteins that contain domain VI motifs, namely, laminin chains $\alpha 1$, $\alpha 2$, $\alpha 5$, $\beta 1$, $\beta 2$, $\beta 3$, $\gamma 1$, $\gamma 3$, and netrins. Laminins are the major noncollagenous components of basement membranes, and they are also present in some mesenchymal compartments. Netrins are small diffusable proteins involved in axon guidance. Therefore, the USH2A protein may be a novel extracellular matrix protein (38, 156).

A total of 20 pathogenic mutations have been reported in USH2A patients, namely, 7 nonsense, 7 frameshift, 1 splice site, and 5 missense (of which 4 are in the laminin type VI domain) mutations (3, 38, 156). Interestingly, the 2299delG (previously termed 2314delG) mutation appears particularly frequently, as it has been detected in 25% of a population of Spanish USH2 families (14) and in about

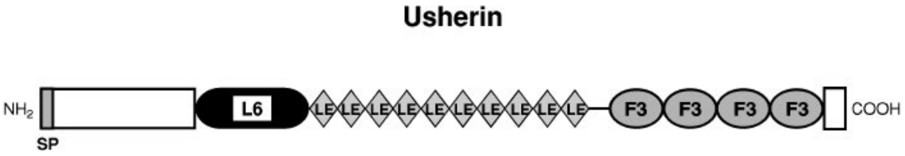

Figure 6 Schematic representation of the *USH2A* encoded protein (usherin). The protein precursor has a signal peptide (SP), which is followed by a 285 amino acid unclassified domain, a laminin domain VI-like (L6) module, 10 laminin type EGF-like (LE) modules, and 4 fibronectin-like type III (F3) repeats. The C-terminal region (50 amino acids) has no detectable homology.

20% of USH2A families from Europe and the United States (156). Finally, the discovery of 4 different missense mutations in the laminin type VI domain of the USH2A protein marks this region for a potentially critical role in the cochlea and retina.

TOWARD PATHOGENESIS

Some clues for understanding the pathogenesis of a genetically heterogeneous disease can be obtained from the pathohistological anomalies observed in animal models, the expression patterns of the underlying genes, the cellular and subcellular localization of the encoded proteins, and the elucidation of the network of molecular interactions in which these proteins are involved. Because so far the genes causative of Usher syndrome have mainly been cloned by groups working in the field of hereditary deafness, the knowledge acquired about the pathogenesis of the disease relates more to the cochlear than to the retinal dysfunction. Presently, more information is available for USH1B than for USH1C and USH1D. Preliminary results for USH2A are also presented.

Usher 1B

COCHLEAR PHENOTYPE: A PRIMARY SENSORY CELL DEFECT The hair bundle of inner ear sensory cells is a highly organized structure that displays a polarity axis in the plane of the epithelium. This planar polarity also manifests by the coordinated orientation of the hair bundles of the different hair cells. Within a bundle, the stereocilia are arranged in several rows of gradually increasing size, resembling a staircase (Figure 7*A*). The hair bundles have a U, V, or W shape. The kinocilium is located eccentrically at the vertex of the bundle; its position defines the vectorial orientation of the bundle. The hair bundle is also functionally polarized; its deflection in the direction of the kinocilium opens the mechanotransduction channels via the stretching of apical links, called the tip links (see Figure 2), which should gate these channels (59). In the most severely affected

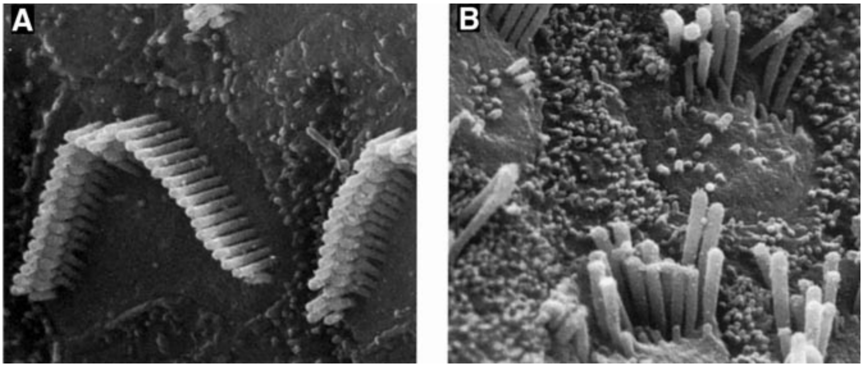

Figure 7 Scanning electron micrographs of the apical surface of auditory hair cells in a wild-type mouse (*A*) and a *shaker-1* mouse (*B*), showing the disorganization of the stereocilia bundle in the mutant lacking a functional myosin VIIA [from Self et al (124)].

sh-1 mouse mutants, the kinocilium is misplaced and the stereocilia display an irregular arrangement (124) (Figure 7*B*). This disorganization of the hair bundle progressively increases after birth; stereocilia form small clumps and splay out (124). Therefore, *sh-1* mutants can be regarded as planar polarity mutants (34). Into this category fall several Drosophila mutants affected in the polarity of hairs, sensory bristles, or ommatidia, which have permitted a genetic dissection of the underlying signaling pathway (99, 116). Erratic positions of the stereocilia are also observed in *mariner* zebrafish mutants (36). Moreover, although hair cells from *sh-1* mice are able to transduce (117, 124), whereas hair cells from *mariner* fishes seem unable to do so (102), this apparent discrepancy may in fact reflect differences in the experimental conditions of this testing because mechanotransduction in *sh-1* mutants requires much greater displacements of the hair bundle than in wild-type animals (76). Therefore, it is reasonable to assume that the disorganization of the hair bundle plays a major role in the hearing loss of USH1B patients. Finally, the hair cells of both *sh-1* mice and *mariner* zebrafish have lost the capacity to accumulate aminoglycosides. Whereas this has been initially interpreted as a defect in an apical endocytic pathway (117, 123), recent results suggest that aminoglycosides may enter the sensory cells via the mechanotransduction channel (G. Richardson, personal communication).

Myosin VIIA is synthesized by numerous cell types; all are epithelial cells that, in most cases, possess microvilli and/or cilia (121). Immunoelectron microscopy has shown that, in these cells, myosin VIIA is present all along the microvilli and the cilia (158). In the mouse inner ear, myosin VIIA is first observed at embryonic day 10 (E10) in the otic vesicle (121). Later, in the cochlea, the protein is restricted to the inner and outer hair cells in all the mammalian species tested (35, 53, 154). It is present in the whole cell body and along the kinocilium (158) and stereocilia

(35, 53, 154). However, the strongest immunoreactivity is associated with the pericuticular necklace; this is a narrow apical region situated between the actin apical belt (associated with the adherens junctions) and the cuticular plate (a dense apical network of horizontal filaments in which the actin filament rootlets of the stereocilia are anchored) (see Figure 2). This region is characterized by the presence of a large pool of coated vesicles (64). In the frog, an intense immunoreactivity has been detected at the base of the stereocilia (52), at the precise emplacements of the ankle links that, in this species, form the major subset of the lateral links that interconnect the stereocilia of the bundle [(44, 133); also see Figure 2].

Recent insight into the function of myosin VIIA at the cellular level provided clues to the understanding of some of the phenotypic anomalies observed in the mouse and zebrafish mutants. *Dictyostelium discoideum* amoeba null mutants for a myosin that may be the orthologue of the mammalian myosin VIIA display impaired phagocytosis (134) and migration, which is related to a defective adhesion to particles and to substrate, respectively (138). Moreover, two ligands of the C-terminal FERM domain of the mammalian myosin VIIA have been characterized. One is the type Iα regulatory subunit of the cAMP-dependent protein kinase (77), which suggests that the activity of myosin VIIA and/or associated molecules could be modulated by cAMP-dependent phosphorylation. The other ligand, vezatin, is a novel ubiquitous transmembrane protein of the adherens junctions (78). Vezatin interacts also with the cadherin-catenin junctional complex, which is involved in cell-cell adhesion and is linked to actin. At the junctions between hair cells and supporting cells (see Figure 2), myosin VIIA, anchored by vezatin, is expected to create a tension force and thus to strengthen cell-cell adhesion (1). The stabilization of these junctions could in turn stabilize the cuticular plate, hence the stereocilia, even though the cuticular plate seems to be attached to the adherens junctions only on the side of the shortest stereocilia (L. Tilney, personal communication). Interestingly, vezatin is also present at the base of the stereocilia, where it is tightly associated with the ankle links (78) (also see Figure 2). By its dynamic activity, the vezatin–myosin VIIA complex at the base of the stereocilia is expected to actively contribute to the cohesion of the hair bundle. Therefore, the loss of a functional vezatin–myosin VIIA complex at both the adherens junctions and the base of the stereocilia is likely to account for the splaying out of the stereocilia observed in myosin VIIA defective animals. Moreover, the presence of myosin VIIA all along the stereocilia in mammals suggests that myosin VIIA also interacts with the other lateral links of the stereocilia (see Figure 2). A possible role at the level of the tip link should also be considered, the loss of which may contribute to the abnormal transduction observed in the myosin VIIA defective mouse and zebrafish mutants (76, 102). Finally, as suggested by the abnormal position of the kinocilium in *sh-1* mice, myosin VIIA at cell-cell junctions might also be implicated in the, as yet undescribed, reorganization and asymetric distribution of the microtubules and microfilaments that should accompany the movement of the kinocilium toward its final peripheral position during the establishment of the planar polarity (55, 136).

RETINAL PHENOTYPE In the mouse retina, myosin VIIA is first detected at E12 in the outer layer of the optic cup, which will give rise to the pigment epithelium cells. Thereafter, the protein is present in both the pigment epithelium cells and the photoreceptor cells in all species tested [although for unclear reasons, some antibodies failed to detect it in the rodent photoreceptors (35)]. Myosin VIIA is localized in the apical processes of the pigment epithelium cells, some of which are involved in the phagocytosis of the outer disks that are exfoliated from the photoreceptors (35, 53, 158) (see Figure 1). In the photoreceptors, the protein is present at the periphery of the connecting cilium, i.e., the slender stalk that joins the inner and outer segments (see Figure 1). Finally, myosin VIIA has also been detected in the synaptic region of chick and macaque photoreceptor cells (35).

No sign of retinal degeneration at any age has ever been observed in the *sh-1* mouse mutants. Recently however, electroretinographic anomalies (a reduction of the amplitude of the wave response to light) have been reported in some *sh-1* mouse mutants carrying a deleterious allele. The pigment epithelium cells have only been examined in a *sh-1* mutant with a mildly deleterious allele. Phagosomes were found to be normal, but the melanosomes did not extend in the apical processes as they did in wild-type mice (85) (Figure 1). In the *sh-1* mice, no morphological anomaly of the photoreceptors has been reported to date (in particular, no misposition of the connecting cilium evoking a polarity defect). However, a significant decrease of the opsin flow at the level of the connecting cilium has been observed (86, 160). Myosin VIIA and actin, which are present along the connecting cilium (159), thus, may participate in the ciliary transport of opsins (86, 160).

The visual loss in retinitis pigmentosa corresponds to the degeneration of photoreceptor cells. The molecular studies have revealed that, in most cases, the primary defects causing these cells to die are either photoreceptor cell or pigment epithelium cell defects (112). Because both cell types express myosin VIIA, the cellular origin of the retinal disease in USH1B cannot be unambiguously established. The defect in melanosome transport in the pigment epithelium cells is not expected to be causative of the USH1B retinal degenerescence (85). However, with respect to the outer disk phagocytosis function of the pigment epithelium cells, the abnormal phagocytosis that has been observed in amoeba null mutants for the putative orthologue of myosin VIIA is intriguing (134).

Usher 1C

Ush1C is transcribed in all the murine tissues tested, with a higher expression in the eye, inner ear, kidney, and small intestine. Immunohistolabeling experiments have shown the presence of harmonin in all the hair cells of the inner ear (143); the protein is detected in the whole cell body and in the stereocilia. In the retina, harmonin is present in the photoreceptor layer (16). Therefore, the cochlear and retinal dysfunctions in USH1C may result from primary sensory cell defects. The various types of cells express different transcripts, with a greater variety in the inner ear than in the eye; moreover, some transcripts predicted to encode b isoforms (see Figure 4) have thus far only been detected in the inner ear. Very little information is available today on the pathogenesis of USH1C because no animal model exists. However, we consider the possibility of an interaction between myosin VIIA and harmonin as an attractive hypothesis, based on the following considerations: (*a*) These proteins, when defective, underlie the same phenotype; (*b*) they colocalize in the same cells, in particular in epithelial cells harboring microvilli; (*c*) PDZ domain–containing proteins are often associated with the sites of cell-cell contacts (80, 94, 99, 116); and (*d*) some PDZ domain–containing proteins interact with proteins of the FERM family (93, 114). The diverse harmonin isoforms predict their involvement in distinct molecular complexes. Major functional information will certainly be obtained from the identification of the transmembrane proteins to which harmonins bind.

Usher 1D

Cdh23 is transcribed in a large variety of murine tissues (19, 33). The gene is highly expressed in the retina. In the inner ear, *Cdh23* expression is restricted to the hair cells (33). In the *waltzer* mutants, the kinocilium is mispositioned, the hair bundle becomes progressively disorganized, and the stereocilia clump together (33), i.e., a series of anomalies resembling those of myosin VIIA defective mutants. Hence, *waltzer* can also be classified as a planar polarity mutant. Interestingly, the Drosophila fat and dachsous cadherins, which belong to the same cadherin subclass as cadherin-23 (161), are involved in epithelial planar polarity (4). Although the cellular distribution of cadherin-23 remains unknown, the usual localization of cadherins at membrane-membrane interacting sites in conjunction with the *waltzer* phenotype argue in favor of a role of cadherin-23 at the junctions with the supporting cells and/or at the level of lateral links. Interestingly, the cadherins present at the junctions between hair cells and supporting cells in the adult mouse have not been characterized yet (79). Moreover, it is noteworthy that in the presence of a calcium chelator, some of the lateral links are proteolyzed (44) and the tip link is disrupted (95). Because cadherins also undergo proteolysis in the absence of calcium (61, 106), cadherins might be components of these links. Because the myosin VIIA ligand vezatin interacts with the cadherin-catenin complex, an exciting possibility is that myosin VIIA and cadherin-23 belong to the same macromolecular complex required to transmit adhesion forces to the cytoskeleton. Arguing in favor of this interaction, double heterozygote *v*/+ *sh-1*/+ mice become deaf at 3 to 6 months of age, whereas *v*/+ and *sh-1*/+ single heterozygote animals have normal hearing (32).

As discussed above, in the absence of a retinal degeneration in USH1B and USH1D mouse models and because of the lack of information on the cellular and/or subcellular localization of vezatin, harmonin, and cadherin-23 in the retina, the pathogenesis of the USH1 retinitis pigmentosa remains highly speculative. However, the absence of retinitis pigmentosa in both the *sh-1* and the *waltzer* deaf mouse mutants argues in favor of the involvement of the *USH1* gene products in a common process in the retina too. Similar to the adhesion defect in the auditory hair cells proposed in USH1, the myosin VIIA signaling pathway may act at some of the membrane-membrane adhesion sites of the photoreceptor cells. These include the synaptic junctions, the junctions with the Müller glial cells, and the contact sites of the calycal process (emerging from the inner segment) (44) with the connecting cilium and the basal part of the outer segment (see Figure 1). A possible role at this latter emplacement should be considered, especially because (*a*) mouse photoreceptor cells lack calycal processes, thus potentially explaining the retinal phenotype discrepancy between humans and mouse, and (*b*) the fibrous links that connect the calycal process to the connecting cilium and outer segment share some molecular components with the lateral links of the hair cells (44).

Usher 2A

No animal model of USH2A is yet available. In situ hybridization studies did not detect the *USH2A* transcript in either the photoreceptor cells or the auditory sensory cells; but rather, it was found in pigment epithelial cells and a variety of epithelial cells of the cochlea, including endothelial cells of the stria vascularis. Immunohistolabeling experiments have revealed usherin as a component of basement membranes in the retina and cochlea (15a). These preliminary data indicate that the cochlear and retinal sensory cells are unlikely to be the primary targets of the USH2A genetic defect.

USH GENES AND ISOLATED DEAFNESS OR RETINITIS PIGMENTOSA

In 1994, the second reported locus responsible for an autosomal recessive form of isolated deafness, DFNB2 (MIM 600060), was mapped to a 6 cM interval overlapping the candidate region for USH1B, through the study of a large consanguineous family living in the central part of Tunisia (49). Thereafter, several other USH loci and DFNB loci were assigned to overlapping genomic regions (see Table 1), namely, USH1C (69) and DFNB18 (MIM 602902) (62), USH1D (149) and DFNB12 (MIM 601386) (25), USH1F (150) and DFNB23 (http://www.uia.ac.be/dnalab/hhh/), USH2B (56) and DFNB6 (MIM 600971) (40), USH3 (122) and DFNB15 (MIM 601869) (26). Moreover, a dominant form of isolated deafness, DFNA11, was also mapped to the same chromosomal region as USH1B and DFNB2. Although this suggested that *USH* genes could also be causative genes for isolated deafness, the candidate intervals initially defined for most of the loci were very large (i.e., exceeded 10 cM). However, it is now established that *MYO7A*, which underlies USH1B, also underlies the isolated forms of deafness DFNB2 (87, 153) and DFNA11 (88). Moreover, strong indication supporting the involvement of *CDH23* and *USH1C* in DFNB12 (19) and DFNB18

(X-Z. Liu, personal communication), respectively, exists. In addition, *USH2A* underlies isolated retinitis pigmentosa (119). Finally, the idea of a continuum between the syndromic and nonsyndromic situations tends to emerge from several recent studies reporting variations of the phenotype within a given family (13, 89, 90, 119).

USH1B and Isolated Deafness

In addition to the aforementioned Tunisian family (49), two small DFNB2 families from China have been identified (87). In the three DFNB2 families, some patients complained of balance problems and/or had abnormal vestibular tests. The hearing loss was severe to profound and congenital in the Chinese families, whereas it was progressive in the Tunisian family (the age of onset ranged from birth to 16 years). Notably, in the Tunisian family, one adult homozygous for the causative mutation had normal hearing. Moreover, a few of the 25 members of this family who carry the biallelic mutation subsequently developed signs of retinal degeneration, whereas others of the same age did not (13). In the Tunisian family, a G>A substitution in the last nucleotide of exon 16 of *MYO7A* was detected (153). This mutation is predicted both to substitute isoleucine for methionine 599 in the motor head of myosin VIIA and to affect the splicing of the mutated exon, resulting in the skipping of this exon in a large proportion of the mature transcripts (151). The expected product of the abnormally spliced transcript is a defective myosin VIIA chain with a 46 amino acid in-frame deletion in the motor head, which might dimerize with the normal chain and thus exert an intra/inter allelic dominant negative effect. One Chinese family was homozygous for the amino acid substitution Arg244Pro located in the motor head of myosin VIIA (87). Affected members of the second Chinese family were compound heterozygotes, who carried a 1 bp insertion in exon 28, leading to the truncation of the tail, on one allele and an acceptor splice site mutation of intron 3 on the other allele (87). Whether the type of the mutation accounts for the expression of either a USH or a DFNB phenotype is difficult to determine. Indeed, on the one hand, in none of the three DFNB2 families do the detected mutations unequivocally predict the complete absence of the protein in the patients. On the other hand, the large phenotypic heterogeneity observed in the Tunisian family, ranging from the lack of any sensory defect to complete Usher syndrome (13), strongly argues in favor of the role of genetic and/or environmental modulating factors. It is noteworthy that the dual sensory dysfunction that was observed in some of the Tunisian patients resembles that of USH3. Along the same line, in one family affected by an atypical Usher syndrome with a progressive hearing loss (i.e., most closely related to USH3), mutations in *MYO7A* have been detected. These patients were compound heterozygotes who carried two missense mutations, namely, a Leu651Pro substitution in the motor head and an Arg1602Gln substitution at the C-terminal end of the first FERM domain (90). As the latter mutation has also been observed in an authentic USH1 family (155), the milder phenotype in this USH3-like family has been proposed to be the result of a genetic background effect (even though the precise impact of the motor head Leu651Pro mutation was unknown) (90).

In the single DFNA11 family reported to date, patients presented with a moderate bilateral hearing loss on all sound frequencies, which appeared in the first decade and then progressed. Vestibular anomalies were detected in some of the individuals. In this family, a 9 bp in-frame deletion located in exon 23, which encodes the coiled-coil domain, was detected (88). The mutated protein may form an inactive dimer with the wild-type myosin VIIA chain (153) and thus have a dominant negative effect. The persistence of some functional wild-type dimers would account for the moderate hearing loss and the absence of retinitis pigmentosa.

In summary, mutations in *MYO7A* can result not only in USH1 but also in USH3-like phenotypes, as well as in dominant or recessive isolated deafness with any degree of severity, congenital or progressive, with or without vestibular dysfunction. So far, no *MYO7A* mutation that leads to isolated retinitis pigmentosa has been discovered, meaning that, for unknown reasons (e.g., a myosin activity with a different critical threshold concentration, a different protein turnover, a cell restricted redundancy, etc.), mutations in myosin VIIA have a more deleterious effect in the inner ear than in the retina. At present, in some cases, the involvement of the genetic background and/or environmental factors in the clinical features can be inferred from distinct phenotypes either present within the same family or associated with the same mutation in different families. In contrast, in the absence of a functional testing of the activity of the various mutated forms of myosin VIIA, the individual effect of a given mutation on the phenotype remains speculative.

USH1D and Isolated Deafness

Whereas only deletions and nonsense or frameshift mutations in *CDH23* have been found in authentic USH1D patients (see above), missense mutations have been detected in several families affected by the isolated form of deafness DFNB12, which is characterized by severe to profound hearing loss (19). Although the entire gene has not yet been explored in these patients, we assume that these mutations are pathogenic. Accordingly, we suggest that the mutation type may play a crucial role in the phenotypic expression of *CDH23* defects. In addition, it is worth noting that the gene encoding protocadherin-15, which is defective in the deaf mouse mutant *Ames waltzer* (5) [which also displays a disorganization of the hair bundle (6)], has been proposed to underlie USH1F and the isolated deafness DFNB23 (5) (see Note Added in Proof, p. 297).

USH2A and Isolated Retinitis Pigmentosa

The *USH2A* 2299delG mutation is present at the homozygous state not only in typical USH2 patients, but also in USH3-like patients who present late onset progressive deafness that is occasionally associated with vestibular dysfunction (89).

The genetic background is not the only source of these differences because they were also observed in monozygotic twins (89). In addition, this mutation has also been detected at the heterozygous state in 4% of patients affected by a recessive form of isolated retinitis pigmentosa who only in the second instance reported mild subjective hearing impairment (119). Finally, a Cys759Phe missense mutation in the fifth LE motif of usherin has been observed in about 4.5% of the cases of recessive retinitis pigmentosa without an auditory defect in North America (119). These patients were either homozygotes for the mutation or compound heterozygotes for one of the aforementioned microdeletions detected in USH2 patients (38). Therefore, mutations in *USH2A* may account for a substantial proportion (i.e., more than 4.5%) of isolated retinitis pigmentosa (119).

CONCLUDING REMARKS

From the recent progress made in characterizing the molecular bases of Usher syndrome, some new ideas are currently emerging about the pathogenesis of this clinically and genetically heterogeneous disorder. Three of them deserve particular mention:

- The results obtained so far on both USH1 B, C, D genetic forms and USH2A indicate that distinct pathogenic processes are likely to account for the different clinical subtypes of the syndrome. In contrast, the various genetic forms of USH1 could result from molecular defects of the same signaling pathway.
- The misposition of the kinocilium during the development of the hair bundle of the auditory sensory cell, which is observed in the mouse models of USH1B and USH1D as well as the anomaly of the connecting cilium of the photoreceptor cell, which has been reported in some USH patients, suggest the existence of a planar polarity defect in USH1. Hence, clarifying USH1 pathogenesis might contribute to the elucidation of the mechanisms involved in the generation of planar polarity in mammals.
- At least three *USH* genes also underlie isolated auditory or visual sensory defects. Moreover, the idea of phenotypic continuums between the syndromic and nonsyndromic situations tends to emerge from several recent reports and to substitute for the classical nosologic frontiers. The analysis of additional mutations in *USH* genes, combined with the study of mutated gene products and careful clinical descriptions, should permit a more accurate estimation of possible direct phenotype-genotype correlation. Perhaps more importantly, these studies should also provide the basis for wide-scale segregation analyses aimed at identifying “modifier genes” in the rest of the genome. From this knowledge, we should gain additional insight into the pathogenic processes involved in Usher syndrome and thereby be guided in the search for targeted therapies.

ACKNOWLEDGMENTS

I am especially grateful to Jean-Pierre Hardelin for his many suggestions to improve the manuscript and to Jacqueline Levilliers for her warm and constant help in the preparation of the manuscript. I thank Aziz El-Amraoui and Sébastien Chardenoux for drawing the figures and Dominic Cosgrove for sharing unpublished results on *USH2A* expression. I also wish to thank Fondation R. & G. Strittmatter (France) and A. & M. Suchert and Forschung contra Blindheit-Initiative Usher Syndrome (Germany) for supporting our research on Usher syndrome.

Visit the Annual Reviews home page at www.AnnualReviews.org

LITERATURE CITED

1. Adams CL, Nelson WJ. 1998. Cytomechanics of cadherin-mediated cell-cell adhesion. *Curr. Opin. Cell Biol.* 10:572–77
2. Adato A, Weil D, Kalinski H, Pel-Or Y, Ayadi H, et al. 1997. Mutation profile of all 49 exons of the human myosin VIIA gene, and haplotype analysis, in Usher 1B families from diverse origins. *Am. J. Hum. Genet.* 61:813–21
3. Adato A, Weston MD, Berry A, Kimberling WJ, Bonné-Tamir A. 2000. Three novel mutations and twelve polymorphisms identified in the USH2A gene in Israeli USH2 families. *Hum. Mutat.* 15:388
4. Adler PN, Charlton J, Liu J. 1998. Mutations in the cadherin superfamily member gene *dachsous* cause a tissue polarity phenotype by altering *frizzled* signaling. *Development* 125:959–68

4a. Ahmed ZM, Riazaddin S, Bernstein SL, Ahmed Z, Khan S, et al. 2001. Mutations of the protocadherin gene *PCDH15* cause Usher syndrome type 1F. *Am. J. Hum. Genet.* 69: In press

5. Alagramam KN, Murcia CL, Kwon HY, Pawlowski KS, Wright CG, et al. 2001. The mouse Ames waltzer hearing-loss mutant is caused by mutation of *Pcdh15*, a novel protocadherin gene. *Nat. Genet.* 27:99–102
6. Alagramam KN, Zahorsky-Reeves J, Wright CG, Pawlowski KS, Erway LC, et al. 2000. Neuroepithelial defects of the inner ear in a new allele of the mouse mutation Ames waltzer. *Hear. Res.* 148:181–91
7. Arden GB, Fox B. 1979. Increased incidence of abnormal nasal cilia in patients with retinitis pigmentosa. *Nature* 279:534–36
8. Astuto LM, Weston MD, Carney CA, Hoover DM, Cremers CWRJ, et al. 2000. Genetic heterogeneity of Usher syndrome: analysis of 151 families with Usher type I. *Am. J. Hum. Genet.* 67:1569–74
9. Auffarth GU, Tetz MR, Krastel H, Blankenagel A, Volcker HE. 1997. Complicated cataracts in various forms of retinitis pigmentosa. Type and incidence. *Ophthalmologe* 94:642–46
10. Ayyagari R, Nestorowicz A, Li Y, Chandrasekharappa S, Chinault C, et al. 1996. Construction of a YAC contig encompassing the Usher syndrome type 1C and familial hyperinsulinism loci on chromosome 11p14-15.1. *Genome Res.* 6:504–14
11. Barrong SD, Chaitin MH, Fliester PS, Possin DE, Jacobson SG, et al. 1982. Ultrastructure of connecting cilia in different forms of retinitis pigmentosa. *Arch. Ophthalmol.* 110:706–10
12. Bell J. 1922. Retinitis pigmentosa and allied diseases. In *Retinitis Pigmentosa and*

Allied Diseases, ed. K Pearson, pp. 1–29. London: Cambridge Press

13. Ben Zina Z, Masmoudi S, Ayadi H, Chaker F, Ghorbel AM, et al. 2001. From DFNB2 to Usher syndrome: variable expressivity of the same disease. *Am. J. Med. Genet.* 101:181–83
14. Beneyto MM, Cuevas JM, Millan JM, Espinos C, Mateu E, et al. 2000. Prevalence of 2314delG mutation in Spanish patients with Usher syndrome type II (USH2). *Ophthalmic Genet.* 21:123–28

14a. Berg JS, Powell BC, Cheney RE. 2000. A millennial myosin census. *Mol. Biol. Cell* 12:780–94

15. Bharadwaj AK, Kasztejna JP, Huq S, Berson EL, Dryja TP. 2000. Evaluation of the myosin VIIA gene and visual function in patients with Usher syndrome type I. *Exp. Eye Res.* 71:173–81

15a. Bhattacharya G, Miller C, Kimberling W, Jablonski MM, Cosgrove D. 2001. Localization and expression of usherin: a novel basement membrane protein defective in people with Usher syndrome type IIa. *Hear. Res.* In press

16. Bitner-Glindzicz M, Lindley KJ, Rutland P, Blaydon D, Smith VV, et al. 2000. A recessive contiguous gene deletion causing infantile hyperinsulinism, enteropathy and deafness identifies the Usher type 1C gene. *Nat. Genet.* 26:56–60
17. Bolz H, von Brederlow B, Ramirez A, Bryda EC, Kutsche K, et al. 2001. Mutations of *CDH23*, encoding a new member of the cadherin gene family, causes Usher syndrome type 1D. *Nat. Genet.* 27:108–12
18. Bonneau D, Raymond F, Kremer C, Klossek J-M, Kaplan J, et al. 1993. Usher syndrome type I associated with bronchiectasis and immotile nasal cilia in two brothers. *J. Med. Genet.* 30:253–54
19. Bork JM, Peters LM, Riazuddin S, Bernstein SL, Ahmed ZM, et al. 2001. Usher syndrome 1D and nonsyndromic autosomal recessive deafness DFNB12 are caused by allelic mutations of the novel cadherin-like gene *CDH23*. *Am. J. Hum. Genet.* 68:26–37
20. Boughman JA, Vernon M, Shaver KA. 1983. Usher syndrome: definition and estimate of prevalence from two high-risk populations. *J. Chronic Dis.* 36:595–603
21. Brix PW, Decher G, von Feilitzsch FCO, Grashof F, Harms F, et al. 1856–1866. *Allgemeine Encyclopädie der Physik*. Leipzig: Leopold Voss
22. Brown KA, Sutcliffe MJ, Steel KP, Brown SDM. 1992. Close linkage of the olfactory marker protein gene to the mouse deafness mutation *shaker-1*. *Genomics* 13:189–93
23. Bryda EC, Ling H, Flaherty L. 1997. A high-resolution genetic map around waltzer on mouse chromosome 10 and identification of a new allele of waltzer. *Mamm. Genome* 8:1–4
24. Chaïb H, Kaplan J, Gerber S, Vincent C, Ayadi H, et al. 1997. A newly identified locus for Usher syndrome type I, *USH1E*, maps to chromosome 21q21. *Hum. Mol. Genet.* 6:27–31
25. Chaïb H, Place C, Salem N, Dodé C, Chardenoux S, et al. 1996. Mapping of DFNB12, a gene for a non-syndromal autosomal recessive deafness, to chromosome 10q21–22. *Hum. Mol. Genet.* 5:1061–64
26. Chen AH, Wayne S, Bell A, Ramesh A, Srisailapathy CRS, et al. 1997. New gene for autosomal recessive non-syndromic hearing loss maps to either chromosome 3q or 19p. *Am. J. Med. Genet.* 71:467–71
27. Chen Z-Y, Hasson T, Kelley PM, Schwender BJ, Schwartz MF, et al. 1996. Molecular cloning and domain structure of human myosin-VIIa, the gene product defective in Usher syndrome 1B. *Genomics* 36:440–48
28. Chishti AH, Kim AC, Marfatia SM, Lutchman M, Hanspal M, et al. 1998. The FERM domain: a unique module involved in the linkage of cytoplasmic

proteins to the membrane. *Trends Biochem. Sci.* 23:281–82

29. Cuevas JM, Espinos C, Millan JM, Sanchez F, Trujillo MJ, et al. 1998. Detection of a novel Cys628STOP mutation of the myosin VIIA gene in Usher syndrome type Ib. *Mol. Cell. Probes* 12:417–20
30. Cuevas JM, Espinos C, Millan JM, Sanchez F, Trujillo MJ, et al. 1999. Identification of three novel mutations in the MYO7A gene. *Hum. Mutat.* 14:181
31. Davenport SLH, Omenn GS. 1977. *The Heterogeneity of Usher Syndrome*. Int. Conf. Birth Defects, Vth, Montreal
32. Deol MS. 1956. The anatomy and development of the mutants pirouette, shaker-1 and waltzer in the mouse. *Proc. R. Soc. London Ser. B* 145:206–13
33. Di Palma F, Holme RH, Bryda EC, Belyantseva IA, Pellegrino R, et al. 2001. Mutations in *Cdh23*, encoding a new type of cadherin, cause stereocilia disorganization in waltzer, the mouse model for Usher syndrome type 1D. *Nat. Genet.* 27:103–7
34. Eaton S. 1997. Planar polarization of *Drosophila* and vertebrate epithelia. *Curr. Opin. Cell Biol.* 9:860–66
35. El-Amraoui A, Sahly I, Picaud S, Sahel J, Abitbol M, et al. 1996. Human Usher IB/mouse *shaker-1*; the retinal phenotype discrepancy explained by the presence/absence of myosin VIIA in the photoreceptor cells. *Hum. Mol. Genet.* 5:1171–78
36. Ernest S, Rauch G-J, Haffter P, Geisler R, Petit C, et al. 2000. *Mariner* is defective in *myosin VIIA*: a zebrafish model for human hereditary deafness. *Hum. Mol. Genet.* 9:2189–96
37. Espinos C, Millan JM, Sanchez F, Beneyto M, Najera C. 1998. Ala397Asp mutation of *myosin VIIA* gene segregating in a Spanish family with type-Ib Usher syndrome. *Hum. Genet.* 102:691–94
38. Eudy JD, Weston MD, Yao S, Hoover DM, Rehm HL, et al. 1998. Mutation of a gene encoding a protein with extracellular matrix motifs in Usher syndrome type IIa. *Science* 280:1753–57
39. Fanning AS, Anderson JM. 1999. PDZ domains: fundamental building blocks in the organization of protein complexes at the plasma membrane. *J. Clin. Invest.* 103:767–72
40. Fukushima K, Ramesh A, Srisailapathy CRS, Ni L, Wayne S, et al. 1995. An autosomal recessive non-syndromic form of sensorineural hearing loss maps to 3p-DFNB6. *Genome Res.* 5:305–8
41. Garner CC, Nash J, Huganir RL. 2000. PDZ domains in synapse assembly and signalling. *Trends Cell Biol.* 10:274–80
42. Gibson F, Walsh J, Mburu P, Varela A, Brown KA, et al. 1995. A type VII myosin encoded by the mouse deafness gene *Shaker-1*. *Nature* 374:62–64
43. Gillespie PG, Wagner MC, Hudspeth AJ. 1993. Identification of a 120 kd hair-bundle myosin located near stereociliary tips. *Neuron* 11:581–94
44. Goodyear R, Richardson G. 1999. The ankle-link antigen: an epitope sensitive to calcium chelation associated with the hair-cell surface and the calycal processes of photoreceptors. *J. Neurosci.* 19:3761–72
45. Gorlin RJ. 1995. Genetic hearing loss associated with eye disorders. See Ref. 46 pp. 105–40
46. Gorlin RJ, Toriello HV, Cohen MM, eds. 1995. *Hereditary Hearing Loss and Its Syndromes*. New York/Oxford: Oxford Univ. Press
47. Gorlin RJ, Tilsner TJ, Feinstein S, Duvall AJD. 1979. Usher's syndrome type III. *Arch. Otolaryngol.* 105:353–54
48. Grondahl J. 1987. Estimation of prognosis and prevalence of retinitis pigmentosa and Usher syndrome in Norway. *Clin. Genet.* 31:255–64
49. Guilford P, Ayadi H, Blanchard S, Chaïb H, Le Paslier D, et al. 1994. A human gene responsible for neurosensory, non-syndromic recessive deafness is a

candidate homologue of the mouse *sh-1* gene. *Hum. Mol. Genet.* 3:989–93
50. Hall RA, Premont RT, Chow CW, Blitzer JT, Pitcher JA, et al. 1998. The beta2-adrenergic receptor interacts with the Na^+/H^+-exchanger regulatory factor to control Na^+/H^+ exchange. *Nature* 392: 626–30
51. Hallgren B. 1959. Retinitis pigmentosa combined with congenital deafness, with vestibulo-cerebellar ataxia and mental abnormality in a proportion of cases. A clinical and genetico-statistical study. In *Acta Psychiatry and Neurologica Scandinavia*, pp. 5–101. Copenhagen: Munksgaard
52. Hasson T, Gillespie PG, Garcia JA, MacDonald RB, Zhao Y, et al. 1997. Unconventional myosins in inner-ear sensory epithelia. *J. Cell Biol.* 137:1287–307
53. Hasson T, Heintzelman MB, Santos-Sacchi J, Corey DP, Mooseker MS. 1995. Expression in cochlea and retina of myosin VIIa, the gene product defective in Usher syndrome type 1B. *Proc. Natl. Acad. Sci. USA* 92:9815–19
54. Hasson T, Walsh J, Cable J, Mooseker MS, Brown SD, et al. 1997. Effects of shaker-1 mutations on myosin-VIIa protein and mRNA expression. *Cell Motil. Cytoskel.* 37:127–38
55. Hirokawa N, Tilney LG. 1982. Interactions between actin filaments and between actin filaments and membranes in quick-frozen and deeply etched hair cells of the chick ear. *J. Cell Biol.* 95:249–61
56. Hmani M, Ghorbel A, Boulila-Elgaïed A, Ben Zina Z, Kammoun W, et al. 1999. A novel locus for Usher syndrome type II, USH2B, maps to chromosome 3 at p 23–24.2. *Eur. J. Hum. Genet.* 7:363–67
57. Hope CI, Bundey S, Proops D, Fielder AR. 1997. Usher syndrome in the city of Birmingham—prevalence and clinical classification. *Br. J. Ophthalmol.* 81:46–53
58. Howard J, Hudspeth AJ. 1987. Mechanical relaxation of the hair bundle mediates adaptation in mechanoelectrical transduction by the bullfrog's saccular hair cell. *Proc. Natl. Acad. Sci. USA* 84:3064–68
59. Hudspeth AJ. 1989. How the ear's works work. *Nature* 341:397–404
60. Hunter DG, Fishman GA, Mehta RS, Kretzer FL. 1986. Abnormal sperm and photoreceptor axonemes in Usher's syndrome. *Arch. Ophthalmol.* 104:385–89
61. Hyafil F, Babinet C, Jacob F. 1981. Cell-cell interactions in early embryogenesis: a molecular approach to the role of calcium. *Cell* 26:447–54
62. Jain PK, Lalwani AK, Li XC, Singleton TL, Smith TN, et al. 1998. A gene for recessive nonsyndromic sensorineural deafness (*DFNB18*) maps to the chromosomal region 11p14-p15.1 containing the Usher syndrome type 1C gene. *Genomics* 50:290–92
63. Janecke AR, Meins M, Sadeghi M, Grundmann K, Apfelststedt-Sylla E, et al. 1999. Twelve novel myosin VIIA mutations in 34 patients with Usher syndrome type I: confirmation of genetic heterogeneity. *Hum. Mutat.* 13:133–40
64. Kachar B, Battaglia A, Fex J. 1997. Compartmentalized vesicular traffic around the hair cell cuticular plate. *Hear. Res.* 107:102–12
65. Kaiser DA, Pollard TD. 1996. Characterization of actin and poly-L-proline binding sites of Acanthamoeba profilin with monoclonal antibodies and by mutagenesis. *J. Mol. Biol.* 256:89–107
66. Kaplan J, Gerber S, Bonneau D, Rozet JM, Delrieu O, et al. 1992. A gene for Usher syndrome type I (USH1A) maps to chromosome 14q. *Genomics* 14:979–87
67. Karjalainen S, Pakarinen L, Terasvirta M, Kaariainen H, Vartiainen E. 1989. Progressive hearing loss in Usher's syndrome. *Ann. Otol. Rhinol. Laryngol.* 98: 863–66
68. Karp A, Santore F. 1983. Retinitis pigmentosa and progressive hearing loss. *J. Speech Hear. Disord.* 48:308–14

69. Keats BJ, Nouri N, Pelias MZ, Deininger PL, Litt M. 1994. Tightly linked flanking microsatellite markers for the Usher syndrome type I locus on the short arm of chromosome 11. *Am. J. Hum. Genet.* 54:681–86
70. Kikuchi K, Hilding DA. 1965. The defective organ of Corti in shaker-1 mice. *Acta Otolaryngol.* 60:287–303
71. Kim E, Niethammer M, Rothschild A, Jan YN, Sheng M. 1995. Clustering of Shaker-type K^+ channels by interaction with a family of membrane-associated guanylate kinases. *Nature* 378:85–88
72. Kimberling WJ, Möller C. 1995. Clinical and molecular genetics of Usher syndrome. *J. Am. Acad. Audiol.* 6:63–72
73. Kimberling WJ, Möller CG, Davenport S, Priluck IA, Beighton PH, et al. 1992. Linkage of Usher syndrome type I gene (USH1B) to the long arm of chromosome 11. *Genomics* 14:988–94
74. Kimberling WJ, Weston MD, Möller C, Davenport SL, Shugart YY, et al. 1990. Localization of Usher syndrome type II to chromosome 1q. *Genomics* 7:245–49
75. Kloepfer HW, Laguaite JK. 1966. The hereditary syndrome of congenital deafness and retinitis pigmentosa. (Usher's syndrome). *Laryngoscope* 76:850–62
76. Kros CJ, Marcotti W, Richardson GP, Brown SDM, Steel KP. 1999. *Electrophysiology of Outer Hair Cells from Myosin VIIA Mutant Mice*. Assoc. Res. Otolaryngol. Meet., Feb. 15, 1999
77. Küssel-Andermann P, El-Amraoui A, Safieddine S, Hardelin J-P, Nouaille S, et al. 2000. Unconventional myosin VIIA is a novel A-kinase anchoring protein. *J. Biol. Chem.* 275:29654–59
78. Küssel-Andermann P, El-Amraoui A, Safieddine S, Nouaille S, Perfettini I, et al. 2000. Vezatin, a novel transmembrane protein, bridges myosin VIIA to the cadherin-catenins complex. *EMBO J.* 19:6020–29
79. Legan PK, Richardson GP. 1997. Extracellular matrix and cell adhesion molecules in the developing inner ear. *Semin. Cell Dev. Biol.* 8:217–24
80. Legouis R, Gansmuller A, Sookhareea S, Bosher JM, Baillie DL, et al. 2000. LET-413 is a basolateral protein required for the assembly of adherens junctions in *Caenorhabditis elegans*. *Nat. Cell Biol.* 2:415–22
81. Lévy G, Levi-Acobas F, Blanchard S, Gerber S, Larget-Piet D, et al. 1997. Myosin VIIA gene: heterogeneity of the mutations responsible for Usher syndrome type IB. *Hum. Mol. Genet.* 6:111–16
82. Lewis RA, Otterud B, Stauffer D, Lalouel JM, Leppert M. 1990. Mapping recessive ophthalmic diseases: linkage of the locus for Usher syndrome type II to a DNA marker on chromosome 1q. *Genomics* 7:250–56
83. Liebreich R. 1861. Abkunft und Ehen unter Blutsverwandten als Grund von Retinitis pigmentosa. *Dtsch. Klin.* 13:53–55
84. Lindenov H. 1945. *The Etiology of Deaf-Mutism with Special Reference to Heredity*. Copenhagen: Munksgaard
85. Liu X, Ondek B, Williams DS. 1998. Mutant myosin VIIa causes defective melanosome distribution in the RPE of shaker-1 mice. *Nat. Genet.* 19:117–18
86. Liu X, Udovichenko IP, Brown SD, Steel KP, Williams DS. 1999. Myosin VIIa participates in opsin transport through the photoreceptor cilium. *J. Neurosci.* 19:6267–74
87. Liu X-Z, Walsh J, Mburu P, Kendrick-Jones J, Cope MJTV, et al. 1997. Mutations in the myosin VIIA gene cause nonsyndromic recessive deafness. *Nat. Genet.* 16:188–90
88. Liu X-Z, Walsh J, Tamagawa Y, Kitamura K, Nishizawa M, et al. 1997. Autosomal dominant non-syndromic deafness caused by a mutation in the myosin VIIA gene. *Nat. Genet.* 17:268–69
89. Liu XZ, Hope C, Liang CY, Zou JM, Xu LR, et al. 1999. A mutation

(2314delG) in the Usher syndrome type IIA gene: high prevalence and phenotypic variation. *Am. J. Hum. Genet.* 64:1221–25

90. Liu XZ, Hope C, Walsh J, Newton V, Ke XM, et al. 1998. Mutations in the myosin VIIA gene cause a wide phenotypic spectrum, including atypical Usher syndrome. *Am. J. Hum. Genet.* 63:909–12
91. Liu XZ, Newton VE, Steel KP, Brown SD. 1997. Identification of a new mutation of the myosin VII head region in Usher syndrome type 1. *Hum. Mutat.* 10:168–70
92. Long RM, Singer RH, Meng X, Gonzalez I, Nasmyth K, et al. 1997. Mating type switching in yeast controlled by asymmetric localization of *ASH1* mRNA. *Science* 277:383–87
93. Lue RA, Brandin E, Chan EP, Branton D. 1996. Two independent domains of hDlg are sufficient for subcellular targeting: the PDZ1-2 conformational unit and an alternatively spliced domain. *J. Cell Biol.* 135:1125–37
94. Mandai K, Nakanishi H, Satoh A, Obaishi H, Wada M, et al. 1997. Afadin: a novel actin filament-binding protein with one PDZ domain localized at cadherin-based cell-to-cell adherens junction. *J. Cell Biol.* 139:517–28
95. Marquis RE, Hudspeth AJ. 1997. Effects of extracellular Ca^{2+} concentration on hair-bundle stiffness and gating-spring integrity in hair cells. *Proc. Natl. Acad. Sci. USA* 94:11923–28
96. Mburu P, Liu XZ, Walsh J, Saw D, Cope MJTV, et al. 1997. Mutation analysis of the mouse myosin VIIA deafness gene. *Genes Funct.* 1:191–203
97. Mermall V, Post PL, Mooseker MS. 1998. Unconventional myosins in cell movement, membrane traffic, and signal transduction. *Science* 279:527–33
98. Metzler WJ, Bell AJ, Ernst E, Lavoie TB, Mueller L. 1994. Identification of the poly-L-proline-binding site on human profilin. *J. Biol. Chem.* 269:4620–25
99. Mlodzik M. 2000. Spiny legs and prickled bodies: new insights and complexities in planar polarity establishment. *Bioessays* 22:311–15
100. Möller CG, Kimberling WJ, Davenport SL, Priluck I, White V, et al. 1989. Usher syndrome: an otoneurologic study. *Laryngoscope* 99:73–79
101. Nguyen JT, Porter M, Amoui M, Miller WT, Zuckermann RN, et al. 2000. Improving SH3 domain ligand selectivity using a non-natural scaffold. *Chem. Biol.* 7:463–73
102. Nicolson T, Rusch A, Friedrich RW, Granato M, Ruppersberg JP, et al. 1998. Genetic analysis of vertebrate sensory hair cell mechanosensation: the zebrafish circler mutants. *Neuron* 20:271–83
103. Nollet F, Kools P, van Roy F. 2000. Phylogenetic analysis of the cadherin superfamily allows identification of six major subfamilies besides several solitary members. *J. Mol. Biol.* 299:551–72
104. Nuutila A. 1970. Dystrophia retinae pigmentosa-dysacusis syndrome (DRD): a study of the Usher or Hallgren syndrome. *J. Genet. Hum.* 18:57–88
105. Deleted in proof
106. Ozawa M, Engel J, Kemler R. 1990. Single amino acid substitutions in one Ca^{2+} binding site of uvomorulin abolish the adhesive function. *Cell* 63:1033–38
107. Pakarinen L, Karjalainen S, Simola KO, Laippala P, Kaitalo H. 1995. Usher's syndrome type 3 in Finland. *Laryngoscope* 105:613–17
108. Piazza L, Fishman GA, Farber M, Derlacki D, Anderson RJ. 1986. Visual acuity loss in patients with Usher's syndrome. *Arch. Ophthalmol.* 104:1336–39
109. Pieke-Dahl S, Moller CG, Kelley PM, Astuto LM, Cremers CW, et al. 2000. Genetic heterogeneity of Usher syndrome type II: localisation to chromosome 5q. *J. Med. Genet.* 37:256–62
110. Pieke-Dahl S, Weston MD, Kimberling WJ. 1997. Genetic heterogeneity of USH. *Am. J. Hum. Genet.* 61(Suppl.):A291

111. Ponting CP. 1997. Evidence for PDZ domains in bacteria, yeast, and plants. *Protein Sci.* 6:464–68
112. Rattner A, Sun H, Nathans J. 1999. Molecular genetics of human retinal disease. *Annu. Rev. Genet.* 33:89–131
113. Raviola E. 1994. The eye. In *A Textbook of Histology*, ed. DW Fawcett, pp. 872–918. New York: Chapman Hall
114. Reczek D, Berryman M, Bretscher A. 1997. Identification of EBP50: a PDZ-containing phosphoprotein that associates with members of the ezrin-radixin-moesin family. *J. Cell Biol.* 139:169–79
115. Reddy AS, Safadi F, Narasimhulu SB, Golovkin M, Hu X. 1996. A novel plant calmodulin-binding protein with a kinesin heavy chain motor domain. *J. Biol. Chem.* 271:7052–60
116. Reifegerste R, Moses K. 1999. Genetics of epithelial polarity and pattern in the *Drosophila* retina. *Bioessays* 21:275–85
117. Richardson GP, Forge A, Kros CJ, Fleming J, Brown SD, et al. 1997. Myosin VIIA is required for aminoglycoside accumulation in cochlear hair cells. *J. Neurosci.* 17:9506–19
118. Rinchik EM, Carpenter DA, Selby PB. 1990. A strategy for fine-structure functional analysis of a 6- to 11-centimorgan region of mouse chromosome 7 by high-efficiency mutagenesis. *Proc. Natl. Acad. Sci. USA* 87:896–900
119. Rivolta C, Sweklo EA, Berson EL, Dryja TP. 2000. Missense mutation in the USH2A gene: association with recessive retinitis pigmentosa without hearing loss. *Am. J. Hum. Genet.* 66:1975–78
120. Rosenberg T, Haim M, Hauch AM, Parving A. 1997. The prevalence of Usher syndrome and other retinal dystrophy-hearing impairment associations. *Clin. Genet.* 51:314–21
121. Sahly I, El-Amraoui A, Abitbol M, Petit C, Dufier J-L. 1997. Expression of myosin VIIA during mouse embryogenesis. *Anat. Embryol.* 196:159–70
122. Sankila E-M, Pakarinen L, Kääriäinen H, Aittomäki K, Karjalainen S, et al. 1995. Assignment of an Usher syndrome type III (USH3) gene to chromosome 3q. *Hum. Mol. Genet.* 4:93–98
123. Seiler C, Nicolson T. 1999. Defective calmodulin-dependent rapid apical endocytosis in zebrafish sensory hair cell mutants. *J. Neurobiol.* 41:424–34
124. Self T, Mahony M, Fleming J, Walsh J, Brown SDM, et al. 1998. Shaker-1 mutations reveal roles for myosin VIIA in both development and function of cochlear hair cells. *Development* 125:557–66
125. Sheng M, Pak DT. 2000. Ligand-gated ion channel interactions with cytoskeletal and signaling proteins. *Annu. Rev. Physiol.* 62:755–78
126. Shieh BH, Zhu MY. 1996. Regulation of the TRP Ca^{2+} channel by INAD in Drosophila photoreceptors. *Neuron* 16:991–98
127. Smith RJH, Berlin CI, Hejtmancik JF, Keats BJB, Kimberling WJ, et al. 1994. Clinical diagnosis of the Usher syndromes. Usher syndrome consortium. *Am. J. Med. Genet.* 50:32–38
128. Smith RJH, Lee EC, Kimberling WJ, Daiger SP, Pelias MZ, et al. 1992. Localization of two genes for Usher syndrome type I to chromosome 11. *Genomics* 14:995–1002
129. Sudol M. 1998. From Src homology domains to other signaling modules: proposal of the ‘protein recognition code.’ *Oncogene* 17:1469–74
130. Deleted in proof
131. Takasaki K, Balaban CD, Sando I. 2000. Histopathologic findings of the inner ears with Alport, Usher and Waardenburg syndromes. *Adv. Oto. Rhino. Laryngol.* 56:218–32
132. Tamayo ML, Bernal JE, Tamayo GE, Frias JL, Alvira G, et al. 1991. Usher syndrome: results of a screening program in Colombia. *Clin. Genet.* 40:304–11
133. Tilney LG, Tilney MS, Cotanche DA. 1988. Actin filaments, stereocilia, and hair

cells of the bird cochlea. V. How the staircase pattern of stereociliary lengths is generated. *J. Cell Biol.* 106:355–65

134. Titus MA. 1999. A class VII unconventional myosin is required for phagocytosis. *Curr. Biol.* 9:1297–303
135. Titus MA, Gilbert SP. 1999. The diversity of molecular motors: an overview. *Cell. Mol. Life Sci.* 56:181–83
136. Troutt LL, van Heumen WR, Pickles JO. 1994. The changing microtubule arrangements in developing hair cells of the chick cochlea. *Hear. Res.* 81:100–8
137. Deleted in proof
138. Tuxworth RI, Weber I, Wessels D, Addicks GC, Soll DR, et al. 2001. A role for myosin VII in dynamic cell adhesion. *Curr. Biol.* 11:318–29
139. Udovichenko IP, Vansant G, Williams DS. 2000. Actin-based motility of baculovirus-expressed and native retinal myosin VIIa. *Mol. Biol. Cell* 11:375 (Abstr. 1944)
140. Usher CH. 1914. On the inheritance of retinitis pigmentosa, with notes of cases. *R. Lond. Ophthalmol. Hosp. Rep.* 19:130–236
141. van Aarem A, Wagenaar M, Tonnaer E, Pieke Dahl S, Bisseling J, et al. 1999. Semen analysis in the Usher syndrome type 2A. *J. Oto-Rhino-Laryngol. Relat. Spec.* 61:126–30
142. Vernon M. 1969. Usher's syndrome—deafness and progressive blindness. Clinical cases, prevention, theory and literature survey. *J. Chronic Dis.* 22:133–51
143. Verpy E, Leibovici M, Zwaenepoel I, Liu X-Z, Gal A, et al. 2000. A defect in harmonin, a PDZ domain–containing protein expressed in the inner ear sensory hair cells, underlies Usher syndrome type 1C. *Nat. Genet.* 26:51–55
144. von Graefe A. 1858. Vereinzelte Beobachtungen und Bemerkungen. Exceptionelle Verhalten des Gesichtsfeldes bei Pigmentenartung des Netzhaut. *Albrecht Graefes Arch. Klin. Ophthalmol.* 4:250–53
145. Wagenaar M. 2000. *The Usher syndrome, a clinical and genetical correlation*. PhD thesis. Univ. Nijmegen, Netherlands
146. Wagenaar M, Schuknecht H, Nadol J Jr, Benraad-Van Rens M, Pieke-Dahl S, et al. 2000. Histopathologic features of the temporal bone in Usher syndrome type I. *Arch. Otolaryngol. Head Neck Surg.* 126:1018–23
147. Wagner HJ. 1997. Presynaptic bodies ("ribbons"): from ultrastructural observations to molecular perspectives. *Cell Tissue Res.* 287:435–46
148. Wang A, Liang Y, Fridell RA, Probst FJ, Wilcox ER, et al. 1998. Association of unconventional myosin *MYO15* mutations with human nonsyndromic deafness *DFNB3*. *Science* 280:1447–51
149. Wayne S, Der Kaloustian VM, Schloss M, Polomeno R, Scott DA, et al. 1996. Localization of the Usher syndrome type 1D gene (Ush1D) to chromosome 10. *Hum. Mol. Genet.* 5:1689–92
150. Wayne S, Lowry RB, McLeod DR, Knaus R, Farr C, et al. 1997. Localization of the Usher syndrome type 1F (Ush1F) to chromosome 10. *Am. J. Hum. Genet.* 61:A300
151. Weil D, Bernard M, Combates N, Wirtz MK, Hollister DW, et al. 1988. Identification of a mutation that causes exon skipping during collagen pre-mRNA splicing in an Ehlers-Danlos syndrome variant. *J. Biol. Chem.* 263:8561–64
152. Weil D, Blanchard S, Kaplan J, Guilford P, Gibson F, et al. 1995. Defective myosin VIIA gene responsible for Usher syndrome type 1B. *Nature* 374:60–61
153. Weil D, Küssel P, Blanchard S, Lévy G, Levi-Acobas F, et al. 1997. The autosomal recessive isolated deafness, DFNB2, and the Usher 1B syndrome are allelic defects of the myosin-VIIA gene. *Nat. Genet.* 16:191–93
154. Weil D, Lévy G, Sahly I, Levi-Acobas F, Blanchard S, et al. 1996. Human myosin VIIA responsible for the Usher 1B syndrome: a predicted membrane-associated

motor protein expressed in developing sensory epithelia. *Proc. Natl. Acad. Sci. USA* 93:3232–37

155. Weston MD, Carney CA, Rivedal SA, Kimberling WJ. 1998. Spectrum of myosin VIIA mutations causing Usher syndrome type Ib. *Assoc. Res. Otolaryngol.* 21:46
156. Weston MD, Eudy JD, Fujita S, Yao S, Usami S, et al. 2000. Genomic structure and identification of novel mutations in usherin, the gene responsible for Usher syndrome type IIa. *Am. J. Hum. Genet.* 66:1199–210
157. Weston MD, Kelley PM, Overbeck LD, Wagenaar M, Orten DJ, et al. 1996. Myosin VIIA mutation screening in 189 Usher syndrome type 1 patients. *Am. J. Hum. Genet.* 59:1074–83
158. Wolfrum U, Liu X, Schmitt A, Udovichenko IP, Williams DS. 1998. Myosin VIIa as a common component of cilia and microvilli. *Cell Motil. Cytoskelet.* 40:261–71
159. Wolfrum U, Schmitt A. 1999. Evidence for myosin VIIa-driven transport of rhodopsin in the plasma membrane of the photoreceptor-connecting cilium. In *Retinal Degenerative Diseases and Experimental Therapy*, ed. JG Hollyfield, pp. 3–14. New York: Kluwer
160. Wolfrum U, Schmitt A. 2000. Rhodopsin transport in the membrane of the connecting cilium of mammalian photoreceptor cells. *Cell Motil. Cytoskelet.* 46:95–107
161. Yagi T, Takeichi M. 2000. Cadherin superfamily genes: functions, genomic organization, and neurologic diversity. *Genes Dev.* 14:1169–80
162. Yonezawa S, Yoshiki A, Hanai A, Matsuzaki T, Matsushima J, et al. 1999. Chromosomal localization of a gene responsible for vestibulocochlear defects of BUS/Idr mice: identification as an allele of waltzer. *Hear. Res.* 134:116–22
163. Zwaenepoel I, Verpy E, Blanchard S, Meins M, Apfelstedt-Sylla E, et al. 2001. Identification of three novel mutations in the USH1C gene and detection of thirty-one polymorphisms used for haplotype analysis. *Hum. Mutat.* 17:34–41

NOTE ADDED IN PROOF

The gene encoding protocadherin15 has just been shown to underlie USH1F (4a).

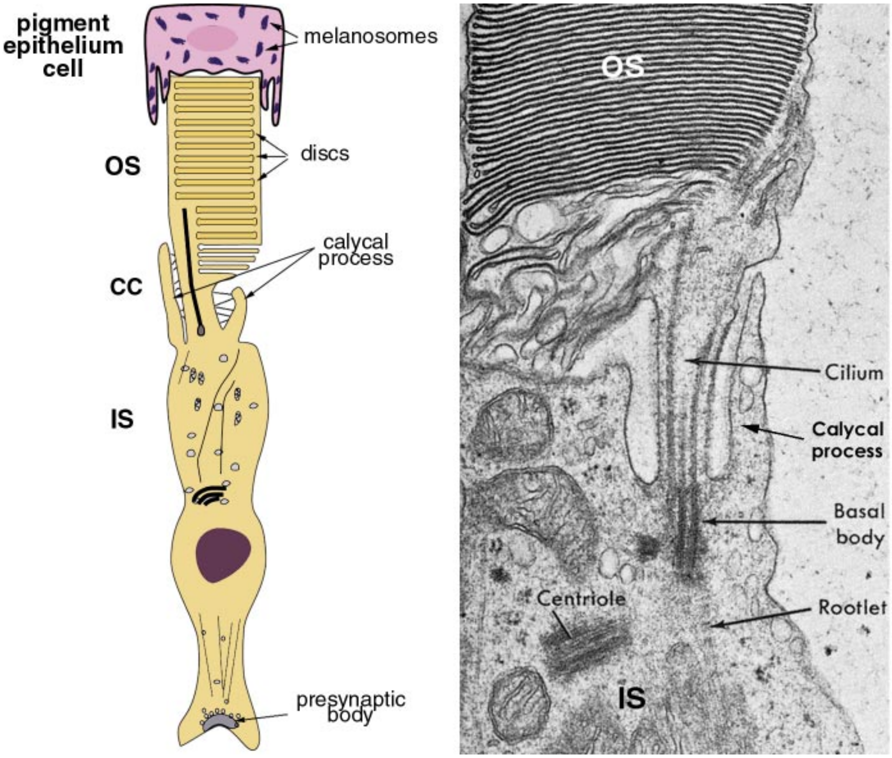
pigment epithelium cell
melanosomes
OS
discs
calycal process
CC
IS
presynaptic body
OS
Cilium
Calycal process
Basal body
Centriole
Rootlet
IS

Figure 1 (*Left*) Schematic representation of a pigment epithelium cell and underlying photoreceptor cell. The photoreceptor cell (here a rod cell) is composed of an outer segment (OS), made up of a large number of discs stacked one above the other (containing the photosensitive molecule rhodopsin), a connecting cilium (CC) (see electron micrograph on the right), and an inner segment (IS) that contains the various cell organelles. The tip of the outer segment (OS) is continually being exfoliated and phagocytized by the overlying pigment epithelium cell. (*Right*) Electron micrograph of a rod cell connecting cilium [from Raviola (113)]. The outer and inner segments of the photoreceptor cell are connected by a modified cilium, which contains nine longitudinally oriented doublet microtubules that arise from a basal body in the end of the inner segment. In human, but not in mouse, the connecting cilium is surrounded by a calycal process.

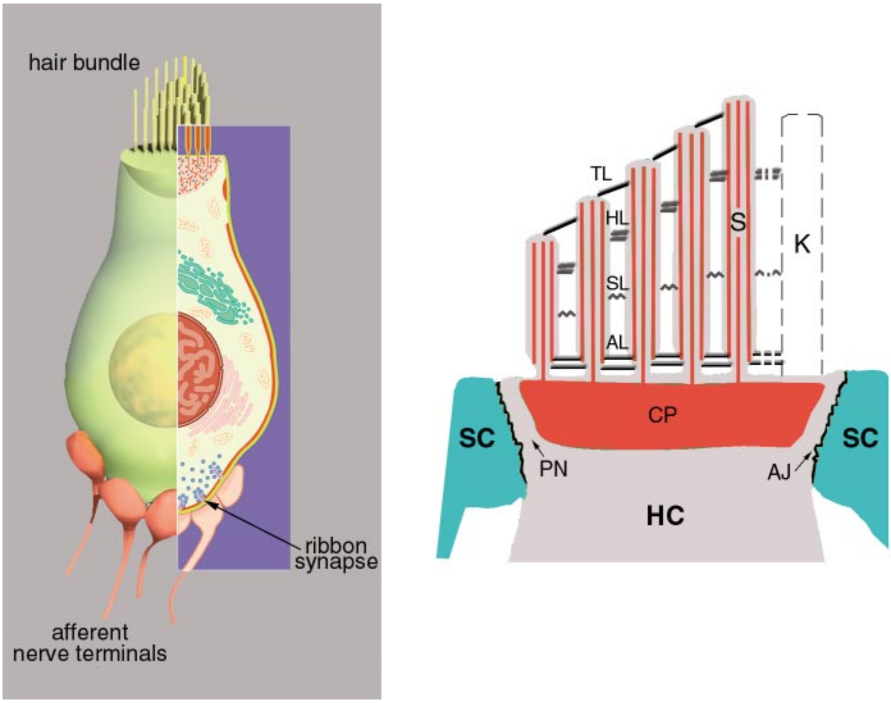

Figure 2 Schematic representation of an auditory inner hair cell (*left*) and detail of the cell apical region (*right*). Note the highly organized hair bundle, made up of several rows of stereocilia (S) at the apical pole of the cell. A stereocilium (K) is located at the vertex of the bundle during cell differentiation; it is no longer present in mature auditory hair cells. The stereocilia are interconnected by several types of lateral links, namely, the ankle links (AL), shaft links (SL), and horizontal links (HL). In addition, a tip link (TL) connects the apex of each stereocilium to the side of the taller adjacent one; tip links should gate the mechanotransduction channels. Three specific structures of the actin cytoskeleton are shown in red, namely, (*a*) the filaments of the stereocilia; (*b*) the cuticular plate (CP), a dense meshwork of horizontal filaments running parallel to the apical cell surface; and (*c*) the cortical network, beneath the plasma membrane. The tight junctions and adherens junctions (AJ) between the hair cell (HC) and the adjacent supporting cells (SC) are also shown. PN, pericuticular necklace.